Solvent Effect on the Photophysical Properties of the Anticancer Agent Ellipticine

S. Y. Fung,[†] J. Duhamel,[‡] and P. Chen*[,†]

Department of Chemical Engineering and Department of Chemistry, University of Waterloo, 200 University Avenue West, Waterloo, Ontario N2L 3G1, Canada

Received: May 6, 2006; In Final Form: July 21, 2006

This paper investigates how solution conditions, especially solvent polarity and hydrogen bonding, affect the fluorescence of ellipticine, a natural plant alkaloid with anticancer activity. A total of 16 solvents that cover a wide range of polarities were tested. The ultraviolet (UV) absorption and fluorescence emission of ellipticine were found to be solvent dependent. The absorption and emission maximum shifted to higher wavelengths (red shift) with increased solvent polarity. The difference in absorption and emission maximum (Stokes' shift) was large, ∼10 000−11 000 cm^{-1}, in polar solvents (with orientation polarizability $\Delta f > 0.2$) but unusually small, ∼8900 cm^{-1}, in nonpolar solvents (hexane and cyclohexane). Large Stokes' shifts were due to an intramolecular charge transfer (ICT), which was enabled by large solvent polarity and hydrogen bonding of ellipticine with the solvents. Two transitions were found in the Lippert−Mataga plot between (1) nonpolar and semipolar solvents and between (2) semipolar and polar solvents. The first transition reflected the formation of hydrogen bonds between ellipticine and the solvents whereas the second transition indicated that ellipticine underwent an ICT. In addition, the larger extinction coefficients and the longer lifetime of ellipticine obtained in protic solvents were attributed to the formation of stronger hydrogen bonds. The photophysical response of ellipticine to changes in solvent polarity and hydrogen bond formation could be used to infer the location of ellipticine in a heterogeneous medium, namely liposomes in aqueous solution. A relatively large red shift of emission in liposomes indicated that ellipticine may be in a more polar environment with respect to the lipid bilayer, possibly close to the hydrophilic interface.

Introduction

Many anticancer agents have been discovered and developed from natural sources,[1−4] as well as from the understanding of molecular genetics and cancer biology.[5−8] Among them, ellipticine, a natural plant alkaloid, and its derivatives have been found to have anticancer activity since the 1960s.[9−12] They are able to intercalate with DNA and inhibit topoisomerase II, leading to the inhibition of replication of DNA and transcription of RNA. While these compounds exhibit high cytotoxicity against tumor cells,[10,11,13−15] only a few clinical trials of ellipticine and its derivatives were attempted in the 1980s.[11,16−19] This is mainly due to the very low solubility of ellipticine and most of its derivatives in aqueous media and in many organic solvents.[11,20,21] In addition, severe side effects have been observed during clinical trials, including intravascular hemolysis, xerostomia, and the decrease of heart beat.[9,11,16]

Recently, ellipticine and its derivatives have drawn renewed attention as new drug delivery technologies have emerged. Ellipticine could be covalently linked with polymers or peptides to form conjugates with significantly improved solubility.[20,22−25] Such conjugates have the potential to target specific cancer cells, thereby reducing side effects.[23−25] Micelles made of copolymers were also used to deliver ellipticine in vitro, and some promising results were reported.[21,26] More recently, a special class of self-assembling peptides has been found to be a good candidate for carrying and delivering hydrophobic compounds.[27,28] These peptides were found to bind to ellipticine, showing great potential as a carrier of ellipticine.

To characterize how ellipticine is transported to its target, it is useful to establish a relationship between the environment and photophysical properties of ellipticine. This will enable one to monitor the uptake of ellipticine by a given carrier and its release from the carrier to a target site by monitoring the change in absorption and emission spectra, as ellipticine migrates from the microenvironment of the carrier to that of the target site. Unfortunately, only a few scattered studies in the literature have reported the photophysical properties of ellipticine and its derivatives.[9,29−32] Some studies focused on the binding of ellipticine to DNA;[33−35] others monitored the ellipticine fluorescence inside cultured cells.[36−38] These studies provided a limited understanding of the photophysical properties of ellipticine. They are summarized hereafter: Ellipticine exhibits several UV absorption bands between 220 and 400 nm, with an extinction coefficient ranging from 3000 to 79 000 M^{-1} cm^{-1}.[29] The UV absorption and fluorescence emission were found to be highly dependent on solution pH.[29,31,32] Ellipticine exhibits a maximum of fluorescence at 520 nm in water (excitation at 304 nm) but an emission maximum at ∼430 nm in ethanol (excitation at 294 nm). This dramatic spectral shift is attributed to the different structures adopted by ellipticine in different solvents. The protonation of the pyridine-like nitrogen (pK_a 6−7.4)[9,31,33] results in an emission maximum at 520 nm, while the neutral form of ellipticine emits fluorescence at ∼430 nm (Scheme 1).[31] The observation of the neutral form of ellipticine in ethanol and its protonated form in a more polar solvent (water) suggests that one may use the solvatochromic effects exhibited by ellipticine to determine its local environ-

* Corresponding author. E-mail address: p4chen@cape.uwaterloo.ca. Fax: 519-746-4979.
[†] Department of Chemical Engineering.
[‡] Department of Chemistry.

10.1021/jp062778y CCC: $33.50
Published on Web 09/16/2006

SCHEME 1: Different Forms of Ellipticine

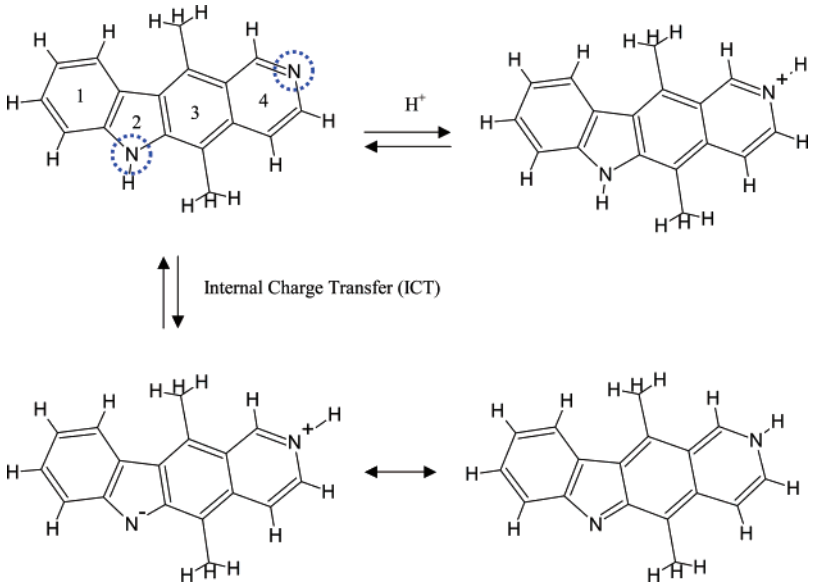

ment, a powerful investigation tool to describe the polarity of a medium in which ellipticine is located. Such a result would be expected to have immediate application to characterize the transfer mechanism of ellipticine in a given delivery system.

In this study, the photophysical properties of ellipticine were determined in a series of organic solvents with different polarities. The UV absorption and fluorescence emission spectra were obtained in each solvent and analyzed in terms of the position of their peak maxima. The position of the peak maxima was correlated to the solvent polarity using the Lippert−Mataga equation.[39,40] The extinction coefficient of ellipticine in each solvent was obtained by applying Beer−Lambert's law. Time-resolved fluorescence experiments were conducted to determine the lifetime of ellipticine. The trends obtained for the absorption and emission of ellipticine as a function of the solvent polarity enable one to use the photophysical properties of ellipticine as a tool to determine its location in a heterogeneous medium. For instance, ellipticine was found to reside close to the surface of the lipid membrane of egg phophatidylcholine (EPC) liposomes.

Experimental Methods

Materials. The solvents (Table 1) were obtained from Sigma-Aldrich (Oakville, Canada), Caledon Laboratories Ltd. (Georgetown, Canada), or EM Science (Gibbstown, NJ) with a purity of 99+%. Dielectric constants (ϵ) and refractive indices (n) of the pure solvents were obtained from the literature.[41] Those of the mixed solvents (ϵ_{mix} and n_{mix}) were estimated from eqs 1 and 2,[42−44]

$$\epsilon_{mix} = f_a\epsilon_a + f_b\epsilon_b \quad (1)$$

$$n_{mix}{}^2 = f_a n_a{}^2 + f_b n_b{}^2 \quad (2)$$

where the subscripts a and b represent the two different pure solvents and $f_{a,b}$ is the volume fraction of each solvent. The polarities of the pure and mixed solvents could be estimated using the definition of the orientation polarizability (Δf) from the Lippert−Mataga equation:[39,40]

$$\Delta f = \frac{\epsilon - 1}{2\epsilon + 1} - \frac{n^2 - 1}{2n^2 - 1} \quad (3)$$

The anticancer agent ellipticine (99.8% pure) was purchased from Sigma-Aldrich (Oakville, Canada) and used without further purification. Egg phosphatidylcholine (EPC) and sodium dodecyl sulfate (SDS) were purchased from Avanti Polar Lipids, Inc. (Alabaster, AL) and EM Science (Gibbstown, NJ), respectively. Ethylenediaminetetraacetic acid (EDTA) was supplied by Bio-Rad Laboratories. Tris(hydroxymethyl)methylamine (Tris) and acetic acid were obtained from BDH Inc. (Toronto, Canada).

Sample Preparation. The ellipticine solutions were prepared from ellipticine stock solutions (100 and 400 μM) in tetrahydrofuran (THF). Aliquots of the ellipticine stock solution (100 μM) in THF were transferred to a 20 mL vial. The vial was then dried under a gentle flow of N_2. Solvents (5 mL) were added to the vial to obtain a solution with a final ellipticine concentration of 2 μM for all fluorescence studies. The same procedure was used to prepare higher ellipticine concentrations (4, 8, 10, and 20 μM) from the 400 μM stock solution for UV absorption experiments. All solutions were degassed prior to performing a steady-state or time-resolved fluorescence experiment.

A 25 mM Tris/acetic acid buffer at pH 7 with 0.2 mM EDTA was used in the dispersions of EPC liposomes. The lipid concentration was determined by taking the difference between the solid content of the vesicle solution and that of the buffer solution. The preparation procedure was described in a previous publication, and the prepared liposomes were characterized as large unilamellar vesicles (LUVs) in terms of their sizes (70−130 nm in diameter).[27] The EPC concentration used in this study equaled 1.1 mM. A 20 mM SDS solution was prepared in ultra pure water (Milli-Q Synthesis, 18.2 MΩ). Liposome dispersions and SDS micelle solutions (5 mL) were added to the sample vial containing a dry film of ellipticine to reach the set 2 μM ellipticine concentration.

UV Absorption. The extinction coefficient of ellipticine at the wavelength corresponding to the absorption maximum in each solvent was determined from the absorption of five ellipticine solutions (2, 4, 8, 10, and 20 μM). The absorption spectra were acquired on a UV−vis spectrophotometer (Biochrom Ultraspec 4300 Pro, Cambridge, England) using a 1 cm path length quartz cell. The molar extinction coefficient (e) was obtained from Beer−Lambert's law where the expression is

TABLE 1: Photophysical Properties of Ellipticine in Different Solvents[a]

solvents	Δf	ϵ	n	λ_a (nm)	ν_a (cm^{-1})	λ_f	ν_f (cm^{-1})	$\nu_a - \nu_f$ (cm^{-1})	e (M^{-1} cm^{-1})
MeOH	0.308	32.70	1.3288	294	34 014	434	23 041	10 972	62 300
ACN	0.305	36.64	1.3442	291.5	34 305	420	23 810	10 495	43 500
EtOH	0.289	24.55	1.3611	294	34 014	429	23 310	10 704	69 900
$Hex_{15}EtOH_{85}$	0.281	21.15	1.3703	294.5	33 956	426	23 474	10 482	
*i*PrOH	0.277	20.18	1.3776	294.5	33 956	424	23 585	10 371	71 300
DMF	0.274	36.70	1.4305	293.5	34 072	425	23 529	10 543	53 600
$Hex_{35}EtOH_{65}$	0.271	16.62	1.3708	294.8	33 921	425	23 529	10 392	
BuOH	0.264	17.50	1.3988	295	33 898	427	23 419	10 479	71 500
DMSO	0.263	46.68	1.4793	295	33 898	428	23 364	10 534	60 000
$Hex_{50}EtOH_{50}$	0.260	13.225	1.3712	295	33 898	423	23 641	10 257	
$Hex_{65}EtOH_{35}$	0.242	9.819	1.3716	295	33 898	422	23 697	10 201	
*t*BuOH	0.238	12.47	1.4255	294.5	33 956	420	23 810	10 146	70 400
$Hex_{75}EtOH_{25}$	0.222	7.552	1.3718	295	33 898	421	23 753	10 145	
THF	0.210	7.520	1.4050	293.3	34 095	413	24 213	9 882	49 600
Hex_1THF_{99}	0.209	7.464	1.4047	293	34 130	412	24 272	9 858	
Hex_5THF_{95}	0.207	7.238	1.4034	293	34 130	412	24 272	9 858	
$Hex_{80}EtOH_{20}$	0.206	6.420	1.3720	294.8	33 921	420	23 810	10 111	
$Hex_{10}THF_{90}$	0.204	6.957	1.4018	293	34 130	411	24 331	9 799	
EAce	0.201	6.081	1.3723	291.5	34 305	410	24 390	9 915	47 400
$Hex_{20}THF_{80}$	0.197	6.393	1.3986	293	34 130	410	24 390	9 740	
$Hex_{30}THF_{70}$	0.188	5.830	1.3954	293	34 130	410	24 390	9 740	
$Hex_{85}EtOH_{15}$	0.185	5.286	1.3721	294.8	33 921	420	23 810	10 111	
*t*AmOH	0.184	5.780	1.4052	294.5	33 956	419	23 867	10 089	70 000
$Hex_{40}THF_{60}$	0.178	5.267	1.3922	293	34 130	409	24 450	9 680	
$Hex_{50}THF_{50}$	0.165	4.703	1.3889	293	34 130	409	24 450	9 680	
ether	0.165	4.267	1.3526	291.5	34 305	405	24 691	9 614	52 100
$Hex_{90}EtOH_{10}$	0.154	4.153	1.3722	294.5	33 956	419	23 866	10 090	
$Hex_{60}THF_{40}$	0.148	4.140	1.3857	292.5	34 188	407	24 570	9 618	
$Hex_{70}THF_{30}$	0.127	3.577	1.3825	292.5	34 188	406	24 631	9 557	
$Hex_{93}EtOH_7$	0.126	3.473	1.3723	294.5	33 956	419	23 866	10 090	
$Hex_{95}EtOH_5$	0.102	3.020	1.3724	294.5	33 956	418	23 923	10 033	
$Hex_{80}THF_{20}$	0.099	3.013	1.3792	292.5	34 188	405	24 691	9 497	
$Hex_{97}EtOH_3$	0.070	2.566	1.3724	294	34 014	418	23 923	10 091	
$Hex_{90}THF_{10}$	0.059	2.450	1.3760	292.5	34 188	403	24 814	9 374	
$Hex_{98}EtOH_2$	0.051	2.340	1.3724	293.3	34 095	416	24 038	10 057	
$Hex_{95}THF_5$	0.033	2.168	1.3743	292	34 247	402	24 876	9 371	
$Hex_{99}EtOH_1$	0.028	2.113	1.3725	291	34 364	407	24 570	9 794	
Diox	0.021	2.219	1.4224	292.5	34 188	410	24 390	9 798	51 800
$Hex_{98}THF_2$	0.014	1.999	1.3734	291.5	34 305	401	24 938	9 367	
Tol	0.013	2.379	1.4961	293	34 130	403	24 814	9 316	47 400
$Hex_{99.6}EtOH_{0.4}$	0.012	1.977	1.3725	290.5	34 423	403	24 814	9 609	
$Hex_{99}THF_1$	0.007	1.943	1.3730	291	34 364	401	24 938	9 426	
$Hex_{99.8}EtOH_{0.2}$	0.006	1.932	1.3725	290.3	34 447	402	24 876	9 571	
CHex	0	2.024	1.4235	290	34 483	392	25 510	8 973	37 700
Hex	0	1.887	1.3727	289.5	34 542	390	25 641	8 901	32 100
EPC				295	33 898	436	22 936	10 962	
SDS				307	32 573	520	19 231	13 342	

[a] Notations: orientation polarizability, Δf; dielectric constant, ϵ; refractive index, n; absorption wavelength, λ_a; absorption wavenumber, ν_a; emission wavelength, λ_f; emission wavenumber, ν_f; extinction coefficient, e. Solvent abbreviation: methanol, MeOH; acetonitrile, ACN; ethanol, EtOH; 2-propanol, *i*PrOH; dimethylforamide, DMF; butanol, BuOH; dimethyl sulfoxide, DMSO; *tert*-butyl alcohol, *t*BuOH; tetrahydrofuran, THF; ethyl acetate, EAce; *tert*-amyl alcohol, *t*AmOH; diethyl ether, ether; 1,4-dioxane, Diox; toluene, Tol; cyclohexane, CHex; hexane, Hex; egg phosphatidylcholine, EPC; sodium dodecyl sulfate, SDS; subscripts for the mixture represent the volume percentage of the two solvents in the mixture (i.e., $Hex_{99}THF_1$: mixture contains 99% hexane and 1% THF). The error for all absorption and emission data is within 0.2%, and that for extinction coefficients is less than 2.0%.

given as[40]

$$\text{absorbance (abs)} = ecd \tag{4}$$

where c is the molar concentration of ellipticine and d is the optical path length (cm). A plot of absorbance versus ellipticine concentration yields a straight line ($R^2 > 0.995$) whose slope equals e, for a 1 cm light path length.

Steady-State and Time-Resolved Fluorescence. All steady-state fluorescence emission spectra were acquired on a Photon Technology International QM-4 spectrofluorometer (London, ON, Canada) with a continuous xenon lamp as the light source. For each sample, approximately 3 mL of solution was transferred from the sample vial into a square quartz cell (1 cm × 1 cm) through a Pasteur glass pipet. The sample was then excited at the wavelength corresponding to the position of the absorption maximum in different solvents (289−305 nm). The emission fluorescence spectra were collected at wavelengths ranging from 300 to 650 nm. Each spectrum was normalized according to its peak maximum. In the case of solutions exhibiting multiple fluorescence peaks, the position of the far left fluorescence peak was used in the Lippert−Mataga equation.

The time-resolved fluorescence decays were acquired on an IBH 5000U time-resolved fluorometer using the time-correlated single photon counting (TCSPC) technique. For each solvent, the excitation was set at the wavelength corresponding to the absorption maximum and the fluorescence was collected at the wavelength corresponding to the fluorescence maximum determined from the steady-state fluorescence spectra. All decay profiles were acquired over 1024 channels, and the data

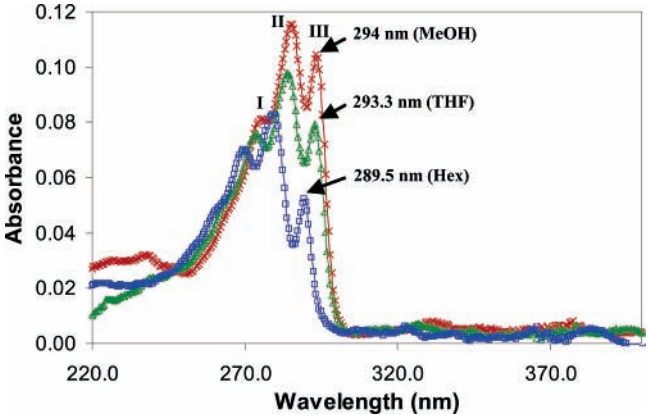

Figure 1. Absorption spectra of ellipticine in hexane (open square), THF (open triangle), and methanol (cross). The ellipticine concentration is 2 μM. The position of peak III was chosen as the excitation wavelength of ellipticine in each solvent.

collection was stopped when the peak maximum reached 20 000 counts. A filter was applied with a cutoff of 370 nm to minimize potential light scattering leaking through the detection system. The decays were then fitted with a mono- or biexponential function, and the fitting parameters were optimized using the Marquardt−Levenberg algorithm.[45] The quality of all fits was determined by the χ^2 parameter, the random distribution of the residuals, and the autocorrelation function of the residuals.

Results and Discussion

Effect of Solvent on the Absorption Spectra. Typical absorption spectra of ellipticine are shown in Figure 1. Ellipticine absorbs over a wide range of wavelengths from 220 to 400 nm. In methanol, three major absorption peaks are found at 294, 285, and 276 nm. The peak locations are very close to the reported values.[29] When ellipticine is in a nonpolar solvent, such as hexane, the absorption spectrum shifts toward the ultraviolet region (blue shift). The 294 nm peak (peak III) in methanol shifts to 289.5 nm in hexane, but it does not change much in the solvents with medium polarity such as THF (absorption spectra for other solvents are not shown). The position of the absorption peak III in all tested solvents is listed in Table 1.

The shift of the absorption spectrum with solvent polarity observed for a solvatochromic compound is a well-known phenomenon. The shift can be described as being hypsochromic or bathochromic depending on whether the absorption maximum occurs at a lower or higher wavelength, respectively. In the case of ellipticine, the absorption spectrum shifts to higher wavelengths with increasing solvent polarity, indicating a bathochromic shift. Normally, the bathochromic shift happens when the dipole moment of the probe (ellipticine in the present case) increases during the electronic transition (i.e., the ground-state dipole moment μ_g < excited-state dipole moment μ_e), and the excited state is formed in a solvent cage of already partly oriented solvent molecules.[46] Thus, more polar solvents favor the stabilization of the excited state of the probe. By examination of the structure of ellipticine (Scheme 1), the electrons are expected to be delocalized between the nitrogen atoms of the pyridine-like ring (ring 4) and of the pyrrole-like ring (ring 2). In addition, hydrogen bonding between the solvent and both nitrogen atoms of ellipticine may induce electron redistribution. This might be the reason, in all protic solvents with strong hydrogen-bonding ability, peak III shifts to higher wavelengths but it remains fixed at low wavelengths in hexane and cyclohexane where the formation of hydrogen bonds is prevented. The effect of specific solvent interactions will be discussed later.

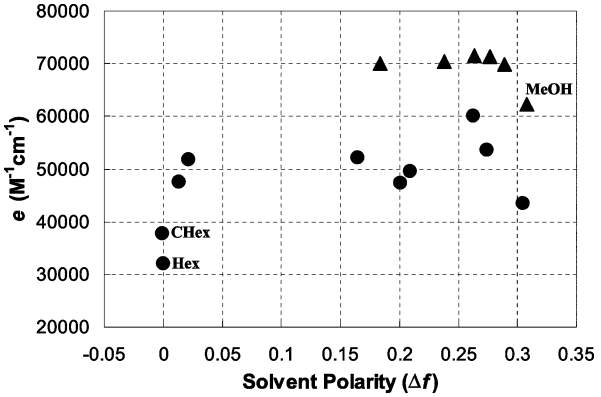

Figure 2. Extinction coefficients of ellipticine as a function of solvent polarity (Δf) (alcohols, triangles). The ellipticine concentrations in hexane and cyclohexane varied from 1 to 5 μM (due to its low solubility in these two solvents), while those in other solvents varied from 2 to 20 μM. The data for each solvent followed a straight line, and the extinction coefficient was obtained through a linear fit of the data using eq 4.

The extinction coefficients (e) at peak III in pure solvents are listed in Table 1 and plotted against the solvent polarity (Δf) in Figure 2. It seems that there is no trend for the extinction coefficients as a function of solvent polarity. The values vary from 32 000 in nonpolar solvents up to ~70 000 in protic solvents (alcohols). Interestingly, ellipticine has the highest extinction coefficients in all protic solvents (solid triangles) except methanol, intermediate ones in aprotic polar solvents, and the lowest ones in nonpolar solvents. This trend seems to follow the hydrogen-bonding ability of the solvents, where the alcohols exhibiting a hydroxyl group (OH) have the strongest hydrogen-bonding ability but the nonpolar solvents cannot form hydrogen bonds with ellipticine. The aprotic polar solvents exhibit either an ether group or an ester group, which can act as hydrogen acceptors for hydrogen bonding, resulting in an intermediate hydrogen-bonding ability. These observations suggest that hydrogen bonding between the solvent and ellipticine affects its extinction coefficient.

Effect of Solvent on the Fluorescence Emission Spectra. Following the absorption experiments, steady-state fluorescence spectra of ellipticine were acquired in the different solvents. A total of 16 organic solvents were tested, and some representative emission spectra are shown in Figure 3. The spectra were normalized with respect to their peak maxima. The peak maximum shifts to the right (red shift) as the solvent polarity increases (from hexane to methanol). Meanwhile, the spectra obtained in apolar solvents such as hexane exhibited several peaks which merged into a single broad peak with increasing solvent polarity. It is worth noting that the emission spectrum in methanol exhibits a red-shifted peak at ~510 nm. This peak is close to the one observed at 520 nm in SDS micelles and aqueous solutions, which has been identified as the protonated form of ellipticine (protonation of the nitrogen on the pyridine-like ring).[31,33,37] This might be due to the fact that methanol, having a smaller pK_a, is more acidic than other alcohols. However, the real mechanisms behind it are still unclear.

Further experiments were conducted to investigate whether the 510 nm peak in methanol could be attributed to the formation of an ellipticine excimer. The fluorescence spectra of a series of ellipticine solutions in methanol with concentrations ranging from 2 to 100 μM were acquired. The ratio of the fluorescence

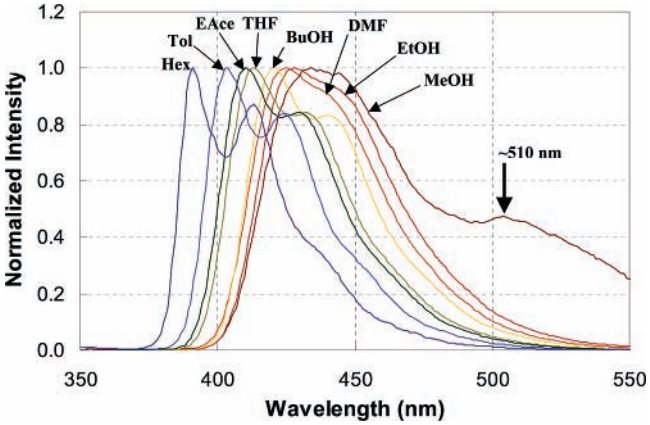

Figure 3. Fluorescence emission spectra of ellipticine (2 μM) in different solvents. All spectra were normalized with respect to the peak maximum.

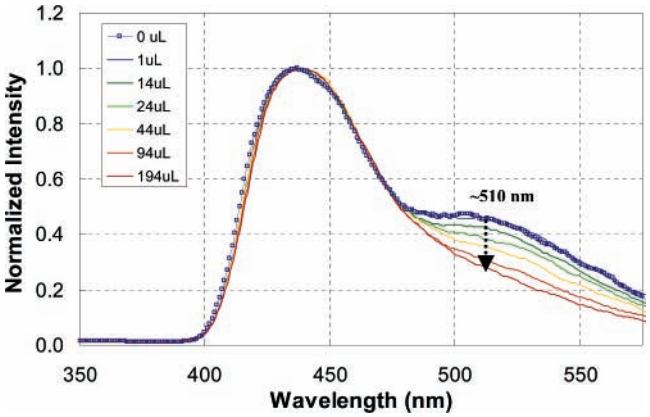

Figure 4. Fluorescence emission spectra of ellipticine (2 μM) in methanol upon addition of 1 M NaOH (top, pure methanol; bottom, 194 μL of 1 M NaOH solution). All spectra were normalized with respect to their peak maxima.

intensity at the 436 nm peak to that at the 510 nm peak was found to remain constant and equal to 2.16 ± 0.02 for all ellipticine concentrations. This result suggests that the 510 nm peak is not due to the formation of an excimer since increasing the ellipticine concentration should have resulted in an increase of the ratio.[47]

To confirm the protonation resulting in the 510 nm peak, a 5 mL methanol solution containing 2 μM ellipticine was titrated by adding 1−194 μL of 1.0 M NaOH solution. As shown in Figure 4, the 510 nm peak decreased with the addition of NaOH due to the deprotonation of ellipticine. Thus, it was concluded that the protonated ellipticine causes the emission peak at ~510 nm in methanol. This result is consistent with the earlier finding that ellipticine is protonated in SDS micelles giving a peak maximum at ~520 nm.[31]

General Solvent Effect and the Lippert−Mataga Relation. The position of the peak maximum (λ_f) for each fluorescence spectrum was plotted against the solvent dielectric constant (ϵ) in Figure 5a and was listed in Table 1. A trend exists where the peak maximum shifts from 390 nm to ~430 nm with increasing solvent dielectric constant. It seems that the profile reaches a plateau when the dielectric constant is larger than 20. Since the dielectric constant is a parameter often taken to represent the solvent polarity, Figure 5a confirms that the solvent polarity affects the fluorescence of ellipticine.

To better understand the solvent polarity effect, the Lippert−Mataga relation was applied. This relation has been widely used to correlate the energy difference between absorption ($h\nu_a$) and

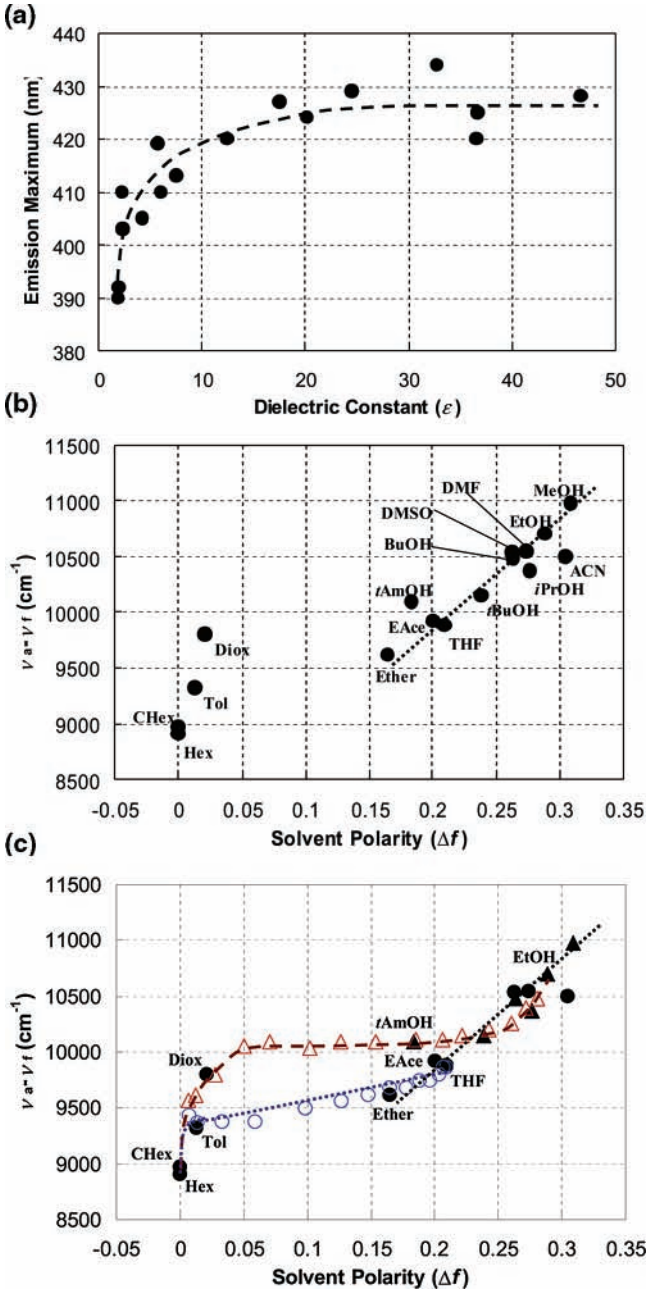

Figure 5. (a) Position of ellipticine fluorescence maximum as a function of solvent dielectric constants. (b) Lippert−Mataga plot of ellipticine in 16 pure solvents. The data are fitted to a straight line (slope = 9700 ± 990, $R^2 > 0.92$) for solvent polarity larger than 0.15. (c) Lippert−Mataga plot of ellipticine in mixtures of hexane−THF (open circles) and hexane−ethanol (open triangles). The ellipticine concentration in each solvent and solvent mixture was set at 2 μM.

emission ($h\nu_f$), also known as Stokes' shift, with solvent polarity represented by Δf. This relation is given in eq 5. It involves both the dielectric constant and the refractive index (n) of the solvents:[39,40]

$$\nu_a - \nu_f = \frac{2}{hc}\left(\frac{\epsilon - 1}{2\epsilon + 1} - \frac{n^2 - 1}{2n^2 + 1}\right)\frac{(\mu_E - \mu_G)^2}{a^3} + \text{const} \quad (5)$$

In eq 5, ν_a and ν_f are the wavenumbers (cm^{-1}) corresponding to the absorption and the emission, respectively, h is Planck's constant, c is the speed of light, and a is the radius of the solvent cavity in which the fluorophore resides. The term involving ϵ and n is called the orientation polarizability (Δf), which only

accounts for the spectral shifts due to the reorientation of the solvent molecules. Therefore, the Lippert−Mataga relation is based on the assumption that the energy difference is only proportional to the solvent orientation polarizability (known as the general solvent effect). Inability of Stokes' shift to increase linearly with Δf usually implies that specific solvent effects are involved.

Figure 5b shows the Lippert−Mataga plot of ellipticine in 16 organic solvents. Stokes' shift increases with increasing solvent polarity. When the solvent polarity (Δf) is larger than 0.15, the data seemed to fall on a straight line. From the Lippert−Mataga equation, the slope of this line yields the dipole moment difference between the ground and excited states, $\Delta\mu$ according to[39,40]

$$\text{slope} = \frac{2(\Delta\mu)^2}{hca^3} \tag{6}$$

The estimated dipole moment difference is 12.2 D (debye) (slope 9700 ± 990, $R^2 > 0.92$), based on the assumption that the Onsager cavity radius a equals 5.35 Å, which is half of the optimized distance between the two farthest atoms of the molecule in the direction of charge separation (10.7 Å).[48] Although this $\Delta\mu$ value was obtained with an approximated cavity radius, it is quite comparable with those reported for other solvatochromic compounds (3−20 D).[48−55] This estimation from the Lippert−Mataga equation is based on the assumption that the photophysical properties of ellipticine can be described by the theory of general solvent effect; hence, it may not hold if specific solvent effects are involved. Actually, Stokes' shifts observed for solvents with a polarity smaller than 0.03 did not follow the trend (Figure 5b). This suggests that the solvent polarity might not be the only factor affecting the spectral shifts. Specific solvent effects including hydrogen bonding, acid−base chemistry, and charge-transfer interactions can also result in nonlinear Lippert−Mataga plots.[40] As mentioned before, ellipticine can form hydrogen bonds with the solvent, and it can shuffle electrons between its two nitrogen atoms (Scheme 1). This complicates the interpretation of how the solvent affects the absorption and emission spectra of ellipticine.

To better understand the factors that affect Stokes' shifts of ellipticine, the data points in Figure 5b can be roughly divided into two groups corresponding to Δf values smaller than 0.03 and larger than 0.15. In the more polar region ($\Delta f > 0.15$), a linear trend was found and the corresponding dipole moment difference was estimated to be 12.2 D. Such a large dipole moment difference usually indicates the occurrence of intramolecular charge transfer (ICT) induced by the solvent after excitation.[48,51−55] Scheme 1 describes the mechanism by which the ICT occurs. In most cases, solvent polarity is believed to be the effect driving an ICT, but for ellipticine, another important factor—hydrogen bonding—should be considered as well. Most solvents used in this study can form hydrogen bonds with ellipticine except hexane and cyclohexane. Alcohols with a hydroxyl group (OH) together with solvents such as DMF and DMSO are expected to form strong hydrogen bonds with ellipticine, which, in addition to their large solvent polarity, may favor the occurrence of an ICT and result in the large 12.2 D dipole moment difference. Although hydrogen bond formation may occur even in less polar solvents such as diethyl ether, THF, and ethyl acetate, the strength of such hydrogen bonds is expected to be weaker;[46] as a result, these solvents will be much less effective at inducing an ICT (see below). In the less polar region ($\Delta f < 0.03$), the data fell on a second, steeper straight line. However, this steeper straight line is probably a coincidence because an ICT should not occur in the nonpolar hexane and cyclohexane where no hydrogen bonds can be formed with ellipticine. In addition, the relatively larger Stokes' shift observed in toluene may be related to the presence of $\pi-\pi$ staking, and that observed in 1,4-dioxane can be due to hydrogen-bonding interactions (see below).

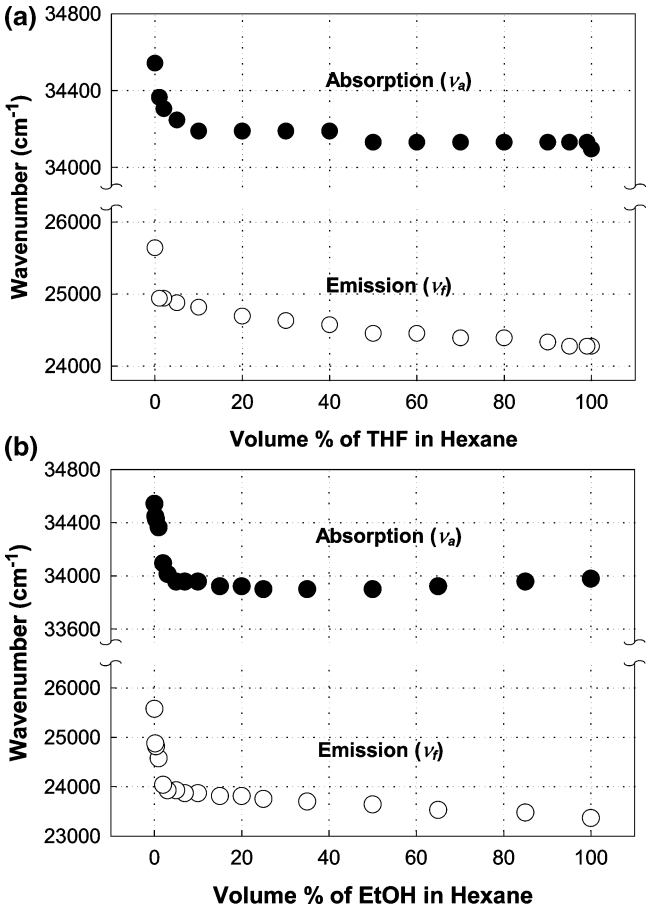

Figure 6. Position of the absorption peak III and emission maximum of ellipticine (2 μM) in (a) hexane−THF mixtures and (b) hexane−ethanol mixtures.

To bridge the gap between the nonpolar ($\Delta f < 0.03$) and semipolar ($0.15 < \Delta f < 0.2$) solvents in the Lippert−Mataga plot, ellipticine solutions were prepared with solvent mixtures of hexane and THF. Such binary mixtures provide a simpler means of studying solvent effects because they reduces the possibilities of specific solvent effects generated by different solvents. The results are listed in Table 1 and plotted in Figure 5c (open circles). Stokes' shifts increase linearly with the solvent polarity, but the mixture containing the lowest volume fraction of THF (1 v/v %) exhibits a Stokes' shift substantially larger than that of hexane. The dramatic increase in Stokes' shift observed for 1 v/v % of THF in hexane cannot be due to an increase of the solvent polarity alone but to specific interactions between THF and ellipticine. This statement is further illustrated in Figure 6a, where the position of the absorption and emission maxima is plotted as a function of solvent composition. Small addition of THF results in a substantial shift of the position of both the absorption and emission maxima.

One possible reason for this effect could be the formation of hydrogen bonds between THF and ellipticine. THF contains an ether function (C−O−C), which can serve as a hydrogen acceptor, so hydrogen bonds can be formed between the NH group on the pyrrole-like ring of ellipticine and the oxygen of

THF. This interaction only requires minute amounts of THF since the ellipticine concentration is very low (2 μM) and that of THF in a 1 v/v % mixture is comparatively high (0.125 M). The presence of minute amounts of THF also affects the absorption of ellipticine (Figure 6a), suggesting that hydrogen bonding between THF and ellipticine must be happening in the ground state.[40,46] When the amount of THF is greater than 5 v/v %, both absorption and emission shift gradually to lower wavenumbers due to the increase of solvent polarity.

In a combination of the data generated from the hexane−THF mixtures with that from 16 pure solvents, a transition is clearly seen at a solvent polarity around 0.2 (Figure 5c). This transition is thought to be an indication that an ICT happens when Δf is above 0.2. However, it is worth noting that the position of this transition is not fixed and depends on different systems of solvent mixtures (see below). Furthermore, solvents with Δf values close to 0.2 (THF, ethyl acetate, and diethyl ether) may be less effective at inducing an ICT as they are very close to the transition region.

The results obtained so far suggest that Stokes' shift of ellipticine in solvents is governed by three factors: solvent polarity; hydrogen bonding; ICT. In the case of solvent mixtures between an alkane and a H-bond-forming solvent, hydrogen bonding is expected to cause a sudden increase of Stokes' shift in nonpolar mixtures followed by a slight increase mainly due to the increase of the mixture polarity ($0.01 < \Delta f < 0.2$); an ICT induced by both hydrogen bonding and solvent polarity occurs when Δf is greater than ~0.2. To validate the transition described above, a series of binary mixtures of hexane and ethanol was prepared, covering a wider range of polarities from 0 to ~0.3. The resulting profile is shown as open triangles in Figure 5c. The previously described transitions are also apparent in this profile. Comparing this profile to that generated with the series of mixtures of hexane and THF, one observes that both display a sudden increase of Stokes' shift upon small addition of the polar cosolvent due to hydrogen bonding, followed by a slight increase for intermediate solvent polarities ($0.05 < \Delta f < 0.2$). When the solvent polarity of the hexane−ethanol mixtures is higher than 0.25, a steeper increase is observed due to an ICT. Overall, the profile obtained from the hexane−ethanol mixtures exhibits a much larger Stokes' shift in the apolar solvent region ($\Delta f < 0.05$) and reflects the occurrence of an ICT in the more polar solvent region ($\Delta f > 0.25$).

The relatively larger Stokes' shift observed with the hexane−ethanol mixtures comparatively to the hexane−THF mixtures is probably due to stronger hydrogen bond formation between ellipticine and ethanol than between ellipticine and THF. This can also be seen by comparing Figure 6a,b. As for THF, the hydrogen bonds were formed in the ground state with the presence of minute amounts of ethanol (less than 5 v/v % in Figure 6b). For Δf values between 0.05 and 0.25, Stokes' shifts remains almost constant regardless of increasing solvent polarity. This result suggests that, in the moderate polarity range, Stokes' shift of ellipticine in the hexane−ethanol mixtures is predominantly determined by hydrogen bonding rather than by solvent polarity. When the polarity is larger than 0.25, ellipticine undergoes an ICT resulting in a large increase of Stokes' shift.

The above discussion rationalizes why some of the data points in Figure 5b (i.e., hexane, cyclohexane, 1,4-dioxane, *tert*-amyl alcohol, and acetonitrile) are scattered and away from the master line obtained for solvents with polarity between 0.15 and 0.32. The nonpolar solvents, hexane and cyclohexane, do not have specific interactions with ellipticine; hence Stokes' shift in these nonpolar solvents is small. A similar observation was reported from Pal and his group when studying coumarin and its derivatives.[56−58] They found that the unusual behavior of coumarin and its derivatives in nonpolar solvents is due to the absence of ICT (i.e., locally excited (LE) state). A much larger Stokes' shift observed in 1,4-dioxane, which is comparable to that obtained with THF and diethyl ether, is probably due to a similar ability of forming hydrogen bonds between ellipticine and the ether oxygen of 1,4-dioxane, THF, or diethyl ether. Similarly, the OH group of *tert*-amyl alcohol may induce stronger hydrogen bonding with ellipticine, so that a larger Stokes' shift than expected from the Δf value is observed. In fact, both 1,4-dioxane and *tert*-amyl alcohol yield Stokes' shifts that fall on the profile generated by the hexane−ethanol mixtures, suggesting the presence of stronger hydrogen bonds between ellipticine and these two solvents. In the region of polar solvents, Stoke's shift of acetonitrile is somewhat lower than its value expected from the linear trend line shown in Figure 5b. This effect may be a result of the weaker hydrogen bonds formed between ellipticine and the CN group than the hydroxyl group (OH) of alcohols, even though acetonitrile is the second most polar solvent in this study.

TABLE 2: Lifetime of Ellipticine in Different Solvents[a]

solvents	Δf	τ_1 (ns)	a_1	τ_2 (ns)	a_2	τ_{avg} (ns)	χ^2
DMSO	0.263	24.4	1.00				1.23
DMF	0.274	25.7	1.00				1.22
$MeOH_{(434)}$	0.308	3.4	0.70	5.3	0.30	4.0	1.10
EtOH	0.289	29.8	1.00				1.21
BuOH	0.264	28.3	1.00				1.10
*t*BuOH	0.238	27.4	1.00				1.16
THF	0.210	21.7	1.00				1.25
EAce	0.201	23.5	1.00				1.19
*t*AmOH	0.184	26.2	1.00				1.22
ether	0.165	15.4	1.00				1.17
Diox	0.021	21.2	1.00				1.15
Tol	0.013	18.3	0.83	13.2	0.17	17.4	1.24
CHex	0	15.1	0.92	4.6	0.08	14.2	1.00
Hex	0	16.5	0.87	4.4	0.13	14.9	1.16
EPC		28.5	0.84	5.8	0.16	24.9	1.19
$MeOH_{(510)}$		9.2	0.89	2.0	−0.11		1.24
SDS		8.5	1.00				1.20

[a] Note: the average lifetime is calculated from eq 7. The subscripts for MeOH represent the wavelengths at which the fluorescence decay was collected.

Solvent Effect on Fluorescence Lifetime. The lifetimes of ellipticine in pure solvents are listed in Table 2. Most decay curves can be well fitted with a single exponential with a χ^2 smaller than 1.3. The others are fitted with a sum of two exponentials. The solvents in which ellipticine has two lifetimes are methanol, toluene, cyclohexane, and hexane. These "abnormal" solvents are either very polar (methanol) or nonpolar (toluene, cyclohexane, and hexane). The data in Table 2 indicate that the lifetime of ellipticine falls in two categories: the longer lifetime ranges from 15 to 29 ns depending on the solvent polarity; the shorter one is around 5 ns. In very polar methanol, ellipticine exhibits a decay time around 3 ns. The reason for the biexponential decay of ellipticine is still unclear. One may speculate that there exist two different forms of ellipticine in methanol, i.e., the protonated and neutral forms as mentioned before; however, such speculation does not hold in nonpolar solvents where two lifetimes are observed because ellipticine cannot be protonated in nonpolar solvents.

The effect of solvent on the lifetimes is illustrated in Figure 7, where the lifetimes are plotted as a function of solvent

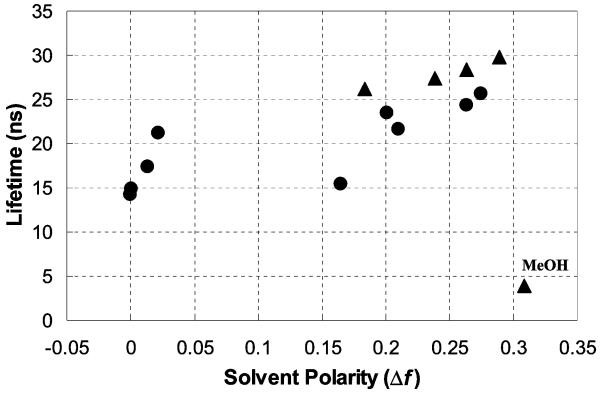

Figure 7. Ellipticine lifetime as a function of solvent polarity. The lifetime increases with increasing solvent polarity. Ellipticine in methanol is an exception with a very short lifetime. Triangles represent alcohols. The ellipticine concentration was set at 2 μM.

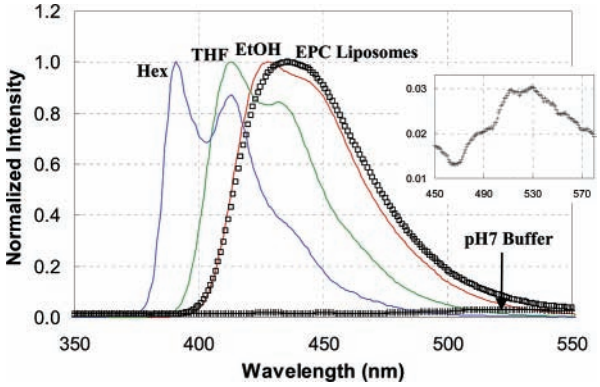

Figure 8. Fluorescence emission spectra of ellipticine (2 μM) in different solvents and EPC liposomes. The spectrum of ellipticine in pH 7 buffer was normalized with respect to the peak maximum in EPC liposomes. The spectrum of ellipticine in buffer is enlarged in the inset.

polarity. When two lifetimes were needed to fit the fluorescence decays, the number average lifetime was calculated with

$$\tau_{avg} = \frac{a_1}{a_1 + a_2}\tau_1 + \frac{a_2}{a_1 + a_2}\tau_2 \qquad (7)$$

where a_1 and a_2 are the contributions of the two decay times obtained from the curve fitting. The average lifetime of ellipticine shown in Figure 7 is scattered between 15 and 30 ns. Interestingly, ellipticine has the longest lifetime in all alcohols (triangles) except in methanol ($\Delta f = 0.308$).

It was shown in Figure 3 that ellipticine exhibits two fluorescence peaks in methanol. To further confirm whether the emission of ellipticine at the 434 and 510 nm peaks came from two different ellipticine species, a fluorescence decay experiment was carried out at 510 nm in addition to 434 nm. The decay time of ellipticine at 510 nm was found to be ~9.2 ns, which is much longer than that at 434 nm (~4.0 ns) (Table 2). Furthermore, the decay acquired at 510 nm displayed a rise time, suggesting that the formation of the species that emitted with a 9.2 ns decay time was delayed. These results clearly show that the fluorescence emission at 434 and 510 nm comes from two different species of ellipticine in methanol. In addition, the species (species II) having a 9.2 ns decay time were formed after those (species I) with a shorter decay time (~4.0 ns) were excited. In fact, the excitation spectra acquired at both emission maxima of 434 and 510 nm overlapped after normalization, which supports the statement that species I of ellipticine is generated prior to species II. The decay time of the protonated form of ellipticine at 520 nm was found to equal ~8.5 ns in SDS micelles, which is comparable to that of ellipticine at 510 nm in methanol. Therefore, these results suggest that the 510 nm fluorescence maximum of ellipticine in methanol is due to the protonated form of ellipticine.

Ellipticine in Lipid Bilayers. The photophysical behavior of ellipticine was investigated in aqueous dispersions of EPC liposomes. Since ellipticine can be qualified as being extremely hydrophobic when considering its very low water solubility (6.2×10^{-7} M),[21] it was expected to reside in the hydrophobic regions of the EPC liposomes. The location of ellipticine in the lipid bilayers might be inferred by comparing the spectral shift of ellipticine in the liposome dispersions with those obtained in organic solvents of known polarity.

The emission spectra of ellipticine in different solvents and in the EPC liposomes were normalized to 1.0 and plotted in Figure 8. The emission band of ellipticine in the liposomes is located at 436 nm ($\lambda_{ex} = 295$ nm), a wavelength very close to that obtained in methanol. The spectrum shows a relatively large red shift, suggesting that a more polar microenvironment is surrounding the ellipticine molecules. For comparison, the fluorescence spectrum of ellipticine in pH 7 Tris/acetic acid buffer solution was acquired. The intensity of this emission spectrum was normalized according to that of ellipticine in EPC liposomes. It is clearly seen that ellipticine in the buffer solution exhibits an emission band at ~520 nm corresponding to its protonated form (Figure 8 inset) and does not dissolve well in aqueous solution resulting in a very low fluorescence signal. These results indicate that the EPC liposomes can efficiently dissolve ellipticine and that the local environment experienced by ellipticine in the liposomes is rather polar and not that expected from ellipticine located inside the hydrophobic lipid bilayer. Consequently, ellipticine dissolved in the liposomes must be located at or close to the interface between the lipid membrane and water. This could be due to the fact that the dipole and quadrupole moments of the indole ring (a combination of rings 1 and 2 in Scheme 1) of ellipticine are more optimal for interacting with charged and polar groups in the phospholipids than with the hydrophobic acyl chains; in addition, the flat rigid shape of ellipticine may limit its access to the hydrocarbon core. Such phenomena have also been found with the amino acid tryptophan (Trp), which consists of an indole ring and has a preference for membrane interfaces.[59] The location of ellipticine at or close to the membrane surface combined with its sensitivity to the local environment suggests that ellipticine might also serve as a surface probe for studying biological phenomena occurring at a membrane interface.

Conclusions

The photophysical properties of the anticancer agent ellipticine were systematically studied in 16 organic solvents and some of their mixtures. The UV absorption and fluorescence emission of ellipticine were found to be solvent dependent. As the solvent polarity increased, ellipticine exhibited a spectral shift to the red for both absorption and emission. The spectral shifts could be correlated with the solvent dielectric constants and the solvent polarity using the Lippert−Mataga equation. The presence of a nonlinear trend in the Lippert−Mataga plot indicated the existence of specific solvent effects. Such effects were thought to result in an intramolecular charge transfer (ICT) due to the large dipole moment difference between the ground state and the excited state. Hydrogen bonding between the solvent and ellipticine can also be related to the specific solvent effects. The formation of stronger hydrogen bonds in alcohols led to

larger extinction coefficients and longer lifetimes, although methanol was an exception. Ellipticine had an emission band at 436 nm in EPC liposomes. The emission band of ellipticine at 436 nm in the liposomes indicated that ellipticine is located in a rather polar environment, certainly close to the hydrophilic surface of the liposomes rather than buried in the hydrophobic interior of the liposome membrane. This study not only provides detailed information on the photophysical properties of ellipticine in many solvents but also suggests that the dependence of the spectral shift of ellipticine with solvent can be a good indicator of where ellipticine is located in a heterogeneous medium like the one offered by EPC liposomes.

Acknowledgment. This research was financially supported by the Natural Sciences and Engineering Research Council of Canada (NSERC), the Canada Research Chairs program, and the Canadian Foundation for Innovation (CFI). We are grateful to Maggie Law for providing help in some absorption experiments and to Mohammad-Reza Asarizadeh for the solvent mixture preparation. We thank Hong Yang for discussions and encouragement.

References and Notes

(1) Singla, A. K.; Grag, A.; Aggarwal, D. *Int. J. Pharm.* **2002**, *235*, 179−192.
(2) Garcia-Carbonero, R.; Supko, J. G. *Clin. Cancer Res.* **2002**, *8*, 641−661.
(3) Srivastava, V.; Negi, A. S.; Kumar, J. K.; Gupta, M. M.; Khanuja, S. P. S. *Bioorg. Med. Chem.* **2005**, *13*, 5892−5908.
(4) Dias, N.; Vezin, H.; Lansiaux, H.; Lansiaux, A.; Bailly, C. *Top. Curr. Chem.* **2005**, *253*, 89−108.
(5) Marks, P. A.; Rifkind, R. A.; Richon, V. M.; Breslow, R.; Miller, T.; Kelly, W. K. *Nat. Rev. Cancer* **2001**, *1*, 194−202.
(6) Adjei, A. A.; Rowinsky, E. K. *Cancer Biol. Ther.* **2003**, *2*, S5−S15.
(7) Moses, M. A.; Brem, H.; Langer, R. *Sci. Med.* **2003**, *9*, 264−273.
(8) Saijo, N.; Tamura, T.; Nishio, K. *Cancer Chemother. Pharmacol.* **2003**, *52* (suppl 1), 97−101.
(9) Garbett, N. C.; Graves, D. E. *Curr. Med. Chem.* **2004**, *4*, 149−172.
(10) Le Pecq, J.-B.; Xuong, N.-D.; Gosse, C.; Paoletti, C. *Proc. Natl. Acad. Sci. U.S.A.* **1974**, *71*, 5078−5082.
(11) Sainsbury, M. In *The Chemistry of Antitumour Agents*; Wilman, D. E. V., Ed.; Blackie and Son Ltd.: Glasgow, U.K., 1990; Chapter 18, pp 411−435.
(12) Ohashi, M.; Oki, T. *Exp. Opin. Ther. Pat.* **1996**, *6*, 1285−1294.
(13) Arteaga, C. L.; Kisner, D. L.; Goodman, A.; Von Hoff, D. D. *Eur. J. Cancer Clin. Oncol.* **1987**, *23*, 1621−1626.
(14) Larue, L.; Rivalle, C.; Muzard, G.; Paoletti, C.; Bisagni, E.; Paoletti, J. *J. Med. Chem.* **1988**, *31*, 1951−1956.
(15) Juret, P.; Tanguy, A.; Le Talaer, J. Y.; Abatucci, J. S.; Dat-Xuong, N.; Le Pecq, J. B.; Paoletti, C. *Eur. J. Cancer* **1978**, *14*, 205−206.
(16) Clarysse, A.; Brugarolas, A.; Siegenthaler, P.; Abele, R.; Cavalli, F.; de Jager, R.; Renard, G.; Rozencweig, M.; Hansen, H. H. *Eur. J. Cancer Clin. Oncol.* **1984**, *20*, 243−247.
(17) Dodion, P.; Rozencweig, M.; Nicaise, C.; Piccart, M.; Cumps, E.; Crespeigne, N.; Kisner, D.; Kenis, Y. *Eur. J. Cancer Clin. Oncol.* **1982**, *18*, 519−522.
(18) Gouyette, A.; Huertas, D.; Droz, J.-P.; Rouesse, J.; Amiel, J.-L. *Eur. J. Cancer Clin. Oncol.* **1982**, *18*, 1285−1292.
(19) Paoletti, C.; Le Pecq, J. B.; Dat-Xuong, N.; Juret, P.; Garnier, H.; Amiel, J.-L.; Rouesse, J. *Recent Res. Cancer Res.* **1980**, *40*, 107−123.
(20) Searle, F.; Gac-Breton, S.; Keane, R.; Dimitrijevic, S.; Brocchini, S.; Sauville, E. A.; Duncan, R. *Bioconjugate Chem.* **2001**, *12*, 711−718.
(21) Liu, J.; Xiao, Y.; Allen, C. *J. Pharm. Sci.* **2004**, *93*, 132−144.
(22) Trubetskoy, V. S.; Torchilin, V. P. *Adv. Drug Delivery Rev.* **1995**, *16*, 311−320.
(23) Czerwinski, G.; Tarasova, N. I.; Michejda, C. J. *Proc. Natl. Acad. Sci. U.S.A.* **1998**, *95*, 11520−11525.
(24) Moody, T. W.; Czerwinski, G.; Tarasova, N. I.; Moody, D. L.; Michejda, C. J. *Regul. Pept.* **2004**, *123*, 187−192.
(25) Moody, T. W.; Czerwinski, G.; Tarasova, N. I.; Michejda, C. J. *Life Sci.* **2002**, *71*, 1005−1014.
(26) Liu, J.; Zeng, F.; Allen, C. *J. Controlled Release* **2005**, *103*, 481−497.
(27) Keyes-Baig, C.; Duhamel, J.; Fung, S. Y.; Bezaire, J.; Chen, P. *J. Am. Chem. Soc.* **2004**, *126*, 7522−7532.
(28) Fung, S. Y.; Hong, Y.; Dhadwar, S. S.; Zhao, X.; Chen, P. In *Handbook of Nanostructured Biomaterials and Their Applications in Nanobiotechnology*; Nalwa, H. S., Ed.; American Scientific Publishers: Stevenson Ranch, CA, 2005; Chapter 1, pp 1−66.
(29) Goodwin, S.; Smith, A. F.; Horning, E. C. *J. Am. Chem. Soc.* **1959**, *81*, 1903−1908.
(30) Terce, F.; Tocanne, J.-F.; Laneelle, G. *Eur. J. Biochem.* **1983**, *133*, 349−354.
(31) Sbai, M.; Ait Lyazidi, S.; Lerner, D. A.; del Castillo, B.; Martin, M. A. *J. Pharm. Biomed. Anal.* **1996**, *14*, 959−965.
(32) Sbai, M.; Lyazidi, S. A.; Lerner, D. A.; del Castillo, B.; Martin, M. A. *Anal. Chim. Acta* **1995**, *303*, 47−55.
(33) El Hage Chahine, J. M.; Bertigny, J.-P.; Schwaller, M.-A. *J. Chem. Soc., Perkin Trans. 2* **1989**, 629−633.
(34) Froelich-Ammon, S. J.; Patchan, M. W.; Osheroff, N.; Thompson, R. B. *J. Biol. Chem.* **1995**, *270*, 14998−15004.
(35) Reha, D.; Kabelac, M.; Ryjacek, F.; Sponer, J.; Sponer, J. E.; Elstner, M.; Suhai, S.; Hobza, P. *J. Am. Chem. Soc.* **2002**, *124*, 3366−3376.
(36) Larsen, A. K.; Paoletti, J.; Belehradek, J., Jr.; Paoletti, C. *Cancer Res.* **1986**, *46*, 5236−5240.
(37) Schwaller, M. A.; Sureau, F.; Turpin, P. Y.; Aubard, J. *J. Lumin.* **1991**, *48 & 49*, 419−424.
(38) Sailer, B. L.; Valdez, J. G.; Steinkamp, J. A.; Darzynkiewicz, Z.; Crissman, H. A. *Exp. Cell Res.* **1997**, *236*, 259−267.
(39) Mataga, N.; Kaifu, Y.; Koizumi, M. *Bull. Chem. Soc. Jpn.* **1956**, *29*, 465−470.
(40) Lakowicz, J. R. *Principles of Fluorescence Spectroscopy*, 2nd ed.; Kluwer Academic/Plenum Publishers: New York, 1999.
(41) *CRC Handbook of Chemistry and Physics, Internet Version 2005*; Lide, D. R., Ed.; CRC Press: Boca Raton, FL, 2005; http://www.hbcpnetbase.com/.
(42) Masuhara, H.; Hino, T.; Mataga, N. *J. Phys. Chem.* **1975**, *79*, 994−1000.
(43) Ghosh, H. N.; Pal, H.; Sapre, A. V.; Mittal, J. P. *J. Am. Chem. Soc.* **1993**, *115*, 11722−11727.
(44) Rath, M. C.; Pal, H.; Mukherjee, T. *J. Phys. Chem. A* **1999**, *103*, 4993−5002.
(45) Press, W. H.; Flannery, B. P.; Teukolsky, S. A.; Vetterling, W. T. *Numerical Resceipes. The Art of Scientific Computing (Fortran Version)*; Cambridge University Press: Cambridge, U.K., 1992; pp 523−528.
(46) Reichardt, C. *Solvents and Solvent Effects in Organic Chemistry*, 2nd ed.; VCH: New York, 1988.
(47) Birks, J. B. *Photophysics of Aromatic Molecules*, Wiley-Interscience: New York, 1970; pp 301−371.
(48) Dey, J.; Warner, I. M. *J. Photochem. Photobiol., A: Chem.* **1998**, *116*, 27−37.
(49) Guzow, K.; Milewska, M.; Wiczk, W. *Spectrochim. Acta, Part A* **2005**, *61*, 1133−1140.
(50) Kitamura, N.; Sakuda, E. *J. Phys. Chem. A* **2005**, *109*, 7429−7434.
(51) Nagy, K.; Gokturk, S.; Biczok, L. *J. Phys. Chem. A* **2003**, *107*, 8784−8790.
(52) Werner, T. C.; Hoffman, R. M. *J. Phys. Chem.* **1973**, *77*, 1611−1615.
(53) Seliskar, C. J.; Brand, L. *J. Am. Chem. Soc.* **1971**, *93*, 5414−5420.
(54) Bosch, P.; Fernandez-Arizpe, A.; Mateo, J. L.; Lozano, A. E.; Noheda, P. *J. Photochem. Photobiol., A: Chem.* **2000**, *133*, 51−57.
(55) Pang, Y. H.; Shuang, S. M.; Wong, M. S.; Li, Z. H.; Dong, C. *J. Photochem. Photobiol., A: Chem.* **2005**, *170*, 15−19.
(56) Nad, S.; Pal, H. *J. Phys. Chem. A* **2001**, *105*, 1097−1106.
(57) Nad, S.; Kumbhakar, M.; Pal, H. *J. Phys. Chem. A* **2003**, *107*, 4808−4816.
(58) Pal, H.; Nad, S.; Kumbhakar, M. *J. Chem. Phys.* **2003**, *119*, 443−452.
(59) Wallace, B. A.; Janes, R. W. *Adv. Exp. Med. Biol.* **1999**, *467*, 789−799.